Business, Management and Economics Engineering
ISSN: 2669-2481 / eISSN: 2669-249X
2023 Volume 21 Issue 02

A NEW MODELING STYRENE POLYMERIZATON IN DIFFERENT SHAPED REACTORS BY USING A NEW MATHEMATICAL METHOD

S.K. Sahani[1],K.S. Prasad[2*], D.N. Mandal[3], K. Sahani[4]
[1*]Department of Mathematics, M.I.T. Campus,T.U., Janakpurdham, Nepal
sureshkumarsahani35@gmail.com
[2*]Department of Mathematics
T.R.M. Campus, T.U., Birgunj, Nepal, kripasinduchaudhary@gmail.com
[3]Department of Mathematics, M.M.C. Campus, T.U., Janakpurdham, Neapl
mandaldevnarayan51@gmail.com
[4]Department of Civil Engineering, Kathmandu University, Dhulikhel, Nepal
kameshwar.sahani@ku.edu.np

Abstract
To tackle the steady three-dimensional equations related to mass, momentum, energy, and species-continuity, the approach of non-orthogonal boundary-fitted coordinate transformation method is employed. Simulating the process of styrene polymerization can benefit from the utilization of this approach, as it enables the calculation of velocity, temperature, and concentration in duct reactors of different geometries. In the model. In this study we take into account how the physical properties of a variable can change, except for specific heat and also include the dissipation of heat due to viscosity and the effects of free convection. However, we do not consider the diffusion that occurs along the axis. The equations for conserving something was first written in a specific type of coordinate system. These equations are changed to have a curved shape in one direction, and then transformed into a different type of coordinate system that can handle different shapes of ducts. The changed equations are divided into small parts called control volumes. These parts are then approximated using specific mathematical methods to calculate the effects of fluid flow and substance transfer. The experiment was done with eight different shapes and we got the outcomes. The results indicate that there isn't one particular shape of the reactor that is consistently better than conventional circular duct reactors in terms of achieving the highest conversion of the chemical reaction. This is true even when taking into account the least amount of pressure loss in the reactors.
Keywords: Boundary-Fitted coordinate, a method of fluid flow ,styrene polymerization, the chemical process ,converting styrene monomers , arbitrary cross-sectional duct reactors, and etc.

INTRODUCTION:

The purpose of this research is to identify a remedy for the transfer of heat and mass in the continuous flow of styrene polymerization within duct reactors that possess diverse cross-sectional shapes. The research done so far on simulating the polymerization of styrene has only focused on traditional cylindrical reactors. Sala and others did the study. By employing numerical methods, we analyzed the polymerization of styrene through equation solving. We used a specific method called the upwind scheme for certain parts of the equations. We also used the stream-function/vorticity approach. The equations that measure the differences

between numbers were solved using a method called Gauss-Seidel. The liquid was thought to follow Newton's laws of fluid behavior. Polystyrene is not a regular fluid. They used physical properties that change with temperature. The thick heat production was ignored. We used a simple process that follows basic rules of chemistry. We also used a specific weight that stays the same and is equal to 70,000 units. We studied how the concentration of the feed, the temperature of the inlet, and the rate at which the feed enters the reactor affect the temperature distribution in both adiabatic and isothermal tubular reactors. It was found that by keeping the temperature of the tube wall lower than the temperature of the substance going into it, the process of making the polymer can be controlled well and prevent it from getting too hot and out of control.

In this article, Wyman and his team describe an approach for estimating the average molecular weights of a particular polymer manufactured in a continuous tubular reactor. The method uses information about the radical and polymer distributions in the reactor. The equations that describe temperature, velocity, and composition were written using a cylindrical tube that has a symmetrical shape and allows for smooth flow with no change in volume. The equations also take into account the varying ability of the substance to flow and conduct heat. The reaction speed was determined using a mathematical formula called the Arrhenius equation. This equation also considers the gel effect.

The decrease in pressure in the tube was calculated using the equation of motion. We did not consider the movement of heat in circles, the heat traveling in a straight line, and the heat created by the friction of the polymer in the equation that determines how much energy is involved. The equation of motion did not consider the speed in different directions. Numbers were employed to solve the partial differential equations through the classical explicit finite-difference method.

Hussain and his team Researchers conducted a computer analysis of how styrene materials combine together in a long, tube-shaped container. They used a mathematical model to represent how the fluid moves inside the container. They thought the polymer did not spread out and ignored speeds going in circles. They also ignored the movement of mass and energy in a straight line. Additionally, they considered the gel effect based on the research done by Hui et al. [4]. Using a method called finite differencing, the equations were solved by breaking them down into smaller parts and solving each part one at a time. This was done by using a specific algorithm called a fourth-order Runge-Kuttab-Gill routine.

Balsamic and others the [5,6] used two different models to understand how styrene is turned into polymer in tube reactors. Tests were done in a really twisted tube that was 14. 6 meters long and had a diameter of 0. 46 centimeters When we heated styrene polymer at 160 degrees Celsius, it turned into something else. This process took about 5. 15 The amount of conversion we achieved was 15%. Chen and other researchers. The investigation of the washout function of residence time was conducted through the use of flow models and tracer techniques. In this text, we are introducing equations that describe how mass, momentum, and energy move in a specific type of flow called laminar antisymmetric flow. We are using cylindrical coordinates

to describe the flow, and we are assuming that the velocity in the direction of flow is fully developed and has a specific shape. We didn't consider the movement of mass and the flow of heat in the same direction. They did not consider the heating caused by the stickiness of the substance. The liquid was expected to behave like a normal liquid. The chemical material was determined to not spread out or move around. The speed at which reactions occur was figured out from Hui et al. study [4], We gathered information about the physical properties from different sources. The method of lines, or MOL, was used to solve the partial differential equations. In this method, the equations were changed into a group of simpler problems called initial value problems, or IVPs, which are ordinary differential equations. Afterwards, the initial value problems (IVPs) were discretized further using finite differences before being resolved using IVP solvers.

The model made calculations about the way things move in a straight line and in a circle. These calculations were then used in a different model that showed how things spread out over time. The answer to this model, when tested at the end of the tube, gave us information about how long it takes for a substance to be washed out of the tube. We did some experiments to check if the theoretical model for how long a substance stays in a space is correct. We used toluene, which doesn't react, as a tracer. The test showed that the velocity profile was stretched. We also figured out the weight of the polymer by using a method that looked at how the radical and polymer were distributed.

Kingstree and Agarwal [9,10] figured out the two-dimensional equations that control the way styrene solidifies when heated in a steady flow inside a straight round tube. They made the assumption that the flow is symmetrical around the tube's axis and that the way the liquid behaves can be described using a power law model. They ignored the force on the body but took into account properties that can change and a flow that starts off with a curved speed pattern. They got the speed rate numbers from Hui et al. And the information about how things look and feel comes from different places. They used a method called control volume approach to divide and analyze the data. They also used a software program that uses the SIMPLE algorithm to get the outcomes. They studied a basic tube to represent the shape of a shell-and-tube configuration. In addition, they used a computer to experiment with different system parameters and found that using a small tube with a radius of up to 2 cm is good for styrene polymerization. However, when the tube gets bigger, it becomes difficult to control temperature increase and keep the flow of material in the tube normal. This makes it impossible to use the tube for its intended purpose. The objective of this research is to employ a particular approach [11] in order to find a solution that facilitates the simulation of the styrene polymerization process in reactors with intricate shapes. We have results for eight different shapes and for five different ways of using them.

THE MATHEMAT ICAL MODELLING

Below, you can find the conservative representation of the equations illustrating the steady continuity in overall, momentum energy, and species.

The Overall Continuity Equation

$$(\nabla.\rho v) = 0 \qquad (1)$$

The Momentum Equation

$$-(\nabla.\rho vv) - \nabla P - (\nabla.\tau) + \rho g = 0 \qquad (2)$$

The Energy Equation

$$-(\nabla.\rho C_P T v) - (\nabla.q) - (\tau : \nabla v) + Q_R = 0 \qquad (3)$$

The Reactant Continuity Equation

$$(\nabla.\rho m_A v) = (\nabla.\rho D_A \nabla m_A) - R_A \qquad (4)$$

The lines that show the directions on a graph are called coordinate axes in Figure 1.

The Constitutive Equation

A mathematical model known as the power-law non-Newtonian model provides a comprehensive explanation for the movement of polystyrene. In the power-law model, the stress-tensor is connected to the rate-of-strain tensor through a specific relationship.

Figure 1. A random-shaped duct in a grid-like system of coordinates.

$$\tau_{ij} = -\mu \left| \sqrt{\frac{1}{2}(\Delta_{ij} : \Delta_{ij}} \right|^{n-1} \Delta_{ij} \qquad (5)$$

The connection between diverse variables in a mathematical equation is clarified through the use of Cartesian Coordinates in the Parabolized Governing Equations. One of these equations, called the continuity equation, describes the overall flow of a substance.

$$\frac{\partial}{\partial x}(\rho u) + \frac{\partial}{\partial y}(\rho v) + \frac{\partial}{\partial z}(pw) = 0 \qquad (6)$$

The Momentum Equations x-Component

$$\frac{\partial}{\partial x}(\rho u^2)+\frac{\partial}{\partial y}(\rho vu)+\frac{\partial}{\partial z}(\rho wu)= -\frac{\partial P}{\partial x}-(\frac{\partial \tau_{xx}}{\partial x}+\frac{\partial \tau_{yx}}{\partial y}) \quad (7)$$

y-Component

$$\frac{\partial}{\partial x}(puv)+\frac{\partial}{\partial y}(pv^2)+\frac{\partial}{\partial z}(pwv)= -\frac{\partial P}{\partial y}-(\frac{\partial \tau_{xy}}{\partial x}+\frac{\partial \tau_{yy}}{\partial y})-(\rho-\rho_a)g \quad (8)$$

z-Component

$$\frac{\partial}{\partial x}(\rho uw)+\frac{\partial}{\partial y}(pvw)+\frac{\partial}{\partial z}(pw^2)= -\frac{d\bar{P}}{dz}-(\frac{\partial \tau_{xz}}{\partial x}+\frac{\partial \tau_{yz}}{\partial y}) \quad (9)$$

The Energy Equation

$$\frac{\partial}{\partial x}(\rho C_P Tu)+\frac{\partial}{\partial y}(\rho C_P Tv)+\frac{\partial}{\partial z}(\rho C_P Tw)= \frac{\partial}{\partial x}(k\frac{\partial T}{\partial x})+\frac{\partial}{\partial y}(k\frac{\partial T}{\partial y})+M.\Phi_v+(-\Delta H)R_A \quad (10)$$

The Reactant Continuity Equation

$$\frac{\partial}{\partial x}(\rho m_A u)+\frac{\partial}{\partial y}(\rho m_A v)+\frac{\partial}{\partial z}(\rho m_A w)= \frac{\partial}{\partial x}(\rho D_A\frac{\partial m_A}{\partial x})+\frac{\partial}{\partial y}(\rho D_A\frac{\partial m_A}{\partial y})-R_A \quad (11)$$

The above equations include the dynamic pressure, P, because of the buoyancy term added to the "y" momentum equation. If the buoyancy effect is not important, P is the total pressure, which is made up of the hydrostatic pressure and the dynamic pressure. The letter M represents how thick a power-law non-Newtonian fluid appears to be.

The Boundary Conditions

Inlet (@z=0) Axial Velocity A uniform entrance velocity profile is specified at inlet:

$$w = w_{inlet} \quad (12)$$

At the entrance of the system, the velocity of the fluid is constant and flows in a straight line.

$$u = 0, \quad v = 0 \quad (13)$$

The temperature is the same throughout and is set at the starting point.

$$T = T_{inlet} \tag{14}$$

Reactant weight fraction refers to the proportion of the reactant that has not been converted into another substance at the beginning of a process or reaction. In simple terms, it is the amount of the starting material that has not been transformed yet.

$$m = 1 \tag{15}$$

The airflow inside the duct is assumed to stick to the walls and not slip.

$$w = 0 \tag{16}$$

Transverse Velocities

$$\mathrm{u} = 0, \qquad \mathrm{v} = 0 \tag{17}$$

When the temperature of a wall stays the same:

$$\mathrm{T} = \mathrm{T}_{\mathrm{wall}} \tag{18}$$

The substance does not pass through the wall.

$$\frac{\partial \mathrm{m}}{\partial \mathrm{n}} = 0 \tag{19}$$

For the equations used here, there is no need for conditions at the end.

THE BOUNDARY-FITTED METHOD

Boundary-fitted coordinate systems revolutionized the way we quantify and chart geographical regions. Instead of using straight lines, we now use curves and shapes that align with the natural boundaries of the area. This eliminates the need to estimate or guess the conditions at these boundaries.

Whether the grid is created orthogonally or non-orthogonally over the physical area determines the nature of the curvilinear coordinate system. In this study, we use a different approach to find answers for the current three-dimensional problem in irregularly-shaped ducts.

TRANSFORMATION OF GOVERNING PDE'S

Before we can break down the partial-differential equations, we need to convert them into different coordinate variables. In general, when we transform something, we make the equations more complicated by adding extra terms to them. The speeds of objects in Cartesian coordinates are kept as the variables that depend on something else in the change. The transformed equations are influenced by the velocity components that experience a reverse change in direction.

The Overall Continuity Equation

$$\frac{\partial}{\partial\zeta}(\rho U)+\frac{\partial}{\partial\eta}(\rho V)+\frac{\partial}{\partial\sigma}(\rho w)=0 \qquad (20)$$

The Momentum Equations x-Component

$$\frac{\partial}{\partial\zeta}(\rho uU)+\frac{\partial}{\partial\eta}(\rho uV)+\frac{\partial}{\partial\sigma}(\rho uW)=$$
$$-\frac{\partial}{\partial\zeta}[y_\eta(\tau_{xx})-x_\eta(\tau_{yx})]-\frac{\partial}{\partial\eta}[x_\zeta(\tau_{yx})-y_\zeta(\tau_{xx})]$$
$$-[y_\eta P_\zeta - y_\zeta P_\eta] \qquad (21)$$

y-Component

$$\frac{\partial}{\partial\zeta}(\rho vU)+\frac{\partial}{\partial\eta}(pvV)+\frac{\partial}{\partial\sigma}(\rho vW)=$$
$$-\frac{\partial}{\partial\zeta}[y_\eta(\tau_{xy})-x_\eta(\tau_{yy})]-\frac{\partial}{\partial\eta}[x_\zeta(\tau_{yy})-y_\zeta(\tau_{xy})]$$
$$-[x_\zeta P_\eta - x_\eta P_\zeta]-J(\rho-\rho_a)g \qquad (22)$$

z-Component

$$\frac{\partial}{\partial\zeta}(\rho wU)+\frac{\partial}{\partial\eta}(pwV)+\frac{\partial}{\partial\sigma}(pwW)=$$
$$-\frac{\partial}{\partial\zeta}[y_\eta(\tau_{xz})-x_\eta(\tau_{yz})]-\frac{\partial}{\partial\eta}[x_\zeta(\tau_{yz})-y_\zeta(\tau_{xz})]$$
$$-J\frac{d\bar{P}}{d\sigma} \qquad (23)$$

The Energy Equation

$$\frac{\partial}{\partial\zeta}(\rho C_p TU)+\frac{\partial}{\partial\eta}(\rho C_p TV)+\frac{\partial}{\partial\sigma}(\rho C_p TW)=$$
$$\frac{\partial}{\partial\zeta}\left[\frac{\alpha}{J}kT_\zeta-\frac{\beta}{J}kT_\eta\right]+\frac{\partial}{\partial\eta}\left[\frac{\gamma}{J}kT_\eta-\frac{\beta}{J}kT_\zeta\right]+$$
$$JM\Phi_v+J(-\Delta H)R_A \qquad (24)$$

The Reactant Continuity Equation

$$\frac{\partial}{\partial\zeta}(\rho m_A U)+\frac{\partial}{\partial\eta}(\rho m_A V)+\frac{\partial}{\partial\sigma}(\rho m_A W)=$$
$$\frac{\partial}{\partial\zeta}\left[\frac{\rho D_A}{J}\alpha m_\zeta-\frac{\rho D_A}{J}\beta m_\eta\right]$$
$$+\frac{\partial}{\partial\eta}\left[\frac{\rho D_A}{J}\gamma m_\eta-\frac{\rho D_A}{J}\beta m_\zeta\right]-J\hat{R}_A \qquad (25)$$

where $m=m_A$ for derivatives.

Boundary Conditions

Inlet (@σ =0)

(i) Axial Velocity $w(\zeta,\eta) = w_{inlet}$ (26)

(ii) Transverse Velocities

$u(\zeta,\eta)0, \quad v(\zeta,\eta) = 0$ (27)

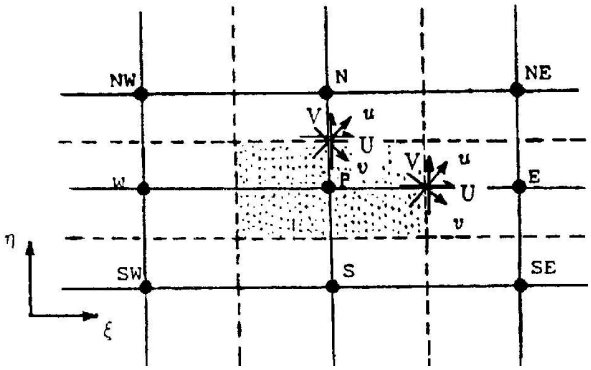

Figure 2. Grid arrangement adopted in Cartesian coordinates (transformed plane).

(iii) Temperature

$T(\zeta,\eta) = T_{inlet}$ (28)

(iv) Reactant Weight-Fraction

$m(\zeta,\eta) = 1.0$ (29)

Walls of the Duct (i) Axial Velocity

$$w(\zeta,\eta) = 0 \quad 1 \le \zeta \le L1 \text{ for } \eta = 1, M_1$$
$$1 \le \eta \le M1 \text{ for } \zeta = 1, L_1 \quad (30)$$

(ii) Transverse Velocities

$$u(\zeta,\eta) = 0 \quad v(\zeta,\eta) = 0 \quad 1 \le \zeta \le L1 \quad \text{for } \eta = 1, M_1$$
$$1 \le \eta \le Ml \quad \text{for } \varepsilon = 1, L_1 \quad (31)$$

(iii) Temperature

$$T(\zeta,\eta) = T_{wall}. \quad 1 \le \zeta \le L1 \quad \text{for } \eta = 1, M_1$$
$$1 \le \eta \le M1 \quad \text{for } \zeta = 1, L_1 \quad (32)$$

(iv) Reactant Weight-Fraction

Note that the transformation parameters are as follows

$$\alpha = x_\eta^2 + y_\eta^2 \qquad U = y_\eta u - x_\eta v$$
$$\beta = x_\zeta x_\eta + y_\varepsilon y_\eta \qquad V = x_\zeta v - y_\zeta u$$
$$\gamma = x_\zeta^2 + y_\zeta^2 \qquad W = Jw$$
$$J = x_\zeta y_\eta - x_\eta y_\xi \quad (33)$$

DISCRETIZATION OF TRANSFORMED EQUATIONS

For a grid system that is not straight, the most effective way to arrange the grid is a changed version of the traditional staggered-grid. One can observe in this configuration that the velocities u and v are employed at the identical point, while the contra-variant velocities run both perpendicular and parallel to the faces of the cell.

The changed governing equations are broken down into smaller parts using a method called the control-volume approach. The upwind difference method is used to divide convective parts into small parts, while the central difference method is used to divide diffusion parts into small parts. The discretization equations are simple math equations that we solve using a traditional matrix algorithm called TDMA. To find the right places for the control-volume faces, we use a type of grid called B-type grid. The SIMPLER algorithm deals with the connection between pressure and velocity in a different direction. It has been changed to work with a specific coordinate system and fluids that do not follow Newton's laws. The way the pressure and velocity are connected in the axial direction in this work is based on the approach used by Rather and Schneider in their work.

TABLE 1. Fluid Properties Data.

Properties	**Correlation**	**Units**
Density Viscosity	$\rho = 1174.7 - 0.918T - (75.3 - 0.313T)W_P$	kg/m^3
	$\mu = \exp[-13.04 - 2013/T - MW^{0.18} - 0$	Pa-s
Thermal Conductivities	$[3.915w_P - 5.437w_P^2 - (0.623 - 1387/T)w_P^3]$	$\frac{J}{(m)(s)(K)}$
	$k_m = [2.72 - 2.8 \times 10^{-3}(T - 150) + 1.6 \times 10^{-5}(T - 150)^2](10^{-4})(418.4)$	$\frac{J}{(m)(s)(K)}$
	$k_P = [2.93 - 5.17 \times 10^{-3}(T - 80)](10^{-4})(418.4)$	$\frac{J}{(m)(s)(K)}$
Specific Heat	$k_{mix} = (1 - X_m)k_m + X_m k_P$	$\frac{J}{kgK_m^2}$
Mass Diffusivity Heat of Reaction	$Cp = 1880.0$	
	$D_m = 2.0 \times 10^{-9}$	$\frac{m^2}{s}$
	$-H = -6.7 \times 10^5$	$\frac{J}{kg}$
Power Law Index	$n = 0.2$	

RESULTS AND DISCUSSION

In this study, we examine how a substance called styrene changes when it gets heated in special reactors with non-round shapes. This reaction [7-10] follows a rate equation that takes into account third-order thermal initiation.

$$R_P = \left(\frac{k_P}{k_t^{\frac{1}{2}}} \right) (2k_i)^{\frac{1}{2}} (M)^{2.5} \quad (34)$$

in which

$$k_i = 2.019 \times 10^1 e^{(-13810/T)} \frac{m^6}{(kg)^2 (s)} \quad (35)$$

$$k_p = 1.009 \times 10^5 e^{(-3557/T)} \frac{m^3}{(kg)(s)} \quad (36)$$

$$k_{tr,m} = 2.218 \times 10^4 e^{(-6377/T)} \frac{m^3}{(kg)(s)} \quad (37)$$

$$k_t = 1.205 \times 10^7 e^{(-844/T)} e^{[-2(A_1 w_P + A_2 w_P^2 + A_3 w_P^3)]} \frac{m^3}{(kg)(s)} \quad (38)$$

Where

$$A_1 = 2.57 - 5.05 \times 10^{-3} T$$
$$A_2 = 9.56 - 1.76 \times 10^{-2} T$$
$$A_3 = -3.03 + 7.85 \times 10^{-3} T - 3.03 \quad (39)$$

The characteristics of the system are displayed in Table 1. The system model and computer codes are checked in sections (i) to (iii) to make sure they are accurate and correct. The results of the previous study and our current study are very similar.

The study does not take into account the influence of free convection, in order to have results that can be compared with existing literature data where this effect is also not considered. More investigations, explained in the next pages, reveal that the impact of free convection on conversion results is very small. The different scenarios can be influenced by altering the number of stations in the axial direction.

Section (i) Husain and Hamelech [3]:

• The tube is 500 centimeters long.
The size of the tube is 2. 0 cm across
The speed of the incoming flow is 0. 0695 centimeters per second.
The temperature of the air coming into the wall is 1000 degrees Celsius and stays at 1000 degrees Celsius.
The conversion rate is 1. 26 weight percent for every 100 centimeters of tube length.
The conversion rate is 3. 95 weight percent for a tube length of 300 centimeters.
The conversion rate is 6. 62 percent by weight for a tube that is 500 centimeters long.

The results obtained in the present analysis areas follows:
(For 5 stations selected in axial direction)

- conversion: 1.38 wt % (for 100 cm tube length)
- conversion: 4.14 wt % (for 300 cm tube length)
- conversion: 6.74 wt % (for 500 cm tube length)(for 10 stations selected in axial direction)
- conversion: 1.37 wt % (for 100 cm tube length)
- conversion: 3.95 wt % (for 300 cm tube length)

conversion: 6.43 wt % (for 500 cm tube length)

These come about are in great assertion with the comes about of Hussain and Hammered [3] who approved their examination by exploratory information of Wallis [3], which included both chemically and thermally, started polymerization of styrene.

Section (ii) Chi-Chi Chen [7]:

- length of tube: 6.4 cm
- tube radius: 0.55 cm
- mass flow: $1.345x1O^{-4}$ kg/sec
- inlet/wall temperature: 140^0C / 135^0C
- conversion: 26.49 wt%.

The result gotten within the show consider is 26.6 wt % change, which is near to the result gotten over.

Section (iii) Kleinstreuer and Agarwal [9]:

- length of tube: 5.0 m
- tube radius: 2 cm
- mass flow: 0.00002 kg/sec
- inlet /wall temperature: $130^0C/100^0C$
- conversion: 54.8 wt %
- velocity profile: parabolic

The comes about gotten within the show ponder are 55.35 wt % and 55.22 wt % for allegorical and uniform speed profiles, separately.

Taking after the approval of the framework modeling and coding system, the concurrent stream, warm and mass exchange issue was fathomed for warm polymerization reactors with distinctive cross-sectional geometries, utilizing 5 sets of working conditions shown in Table 2.

Choosing the shape of ducts and their angles and measurements can have limitless possibilities. However, some basic shapes were chosen because there was no specific preference for choosing a particular one. These arrangements are as shown below:

- circular duct,
- square duct,
- equilateral triangular duct,
- trapezoidal duct (acute angle =60^0, one sidetwice the other),
- pentagonal duct (each angle = 108^0)
- hexagonal duct (each angle = 120^0)
- rectangular duct (aspect ratio 1.5)

rectangular duct (aspect ratio: 2.0)

These shapes are displayed in Figure 3.
To make sure the numbers are accurate and the calculations are efficient, a grid size of 21x21 was chosen sideways. The computer's processing time was around 10 minutes for one operation on an IBM ESA9000 machine. It took about 5 rounds on each changed space for everything to become stable and come together. The criteria for convergence were determined based on the remaining values called residuals.

TABLE 2. Operating Conditions.

Case	W_{inlet}(m/s)	T_{inlet} (^{0}C)	T_{wall} (^{0}C)	Mass-flow(kg/s)	Reactor Length (m)
# 1	0.000695	100	100	0.7267 x $1O^{-3}$	5.0
# 2	0.000695	130	100	0.7027 x $1O^{-3}$	5.0
# 3	0.001780	140	135	0.1345 x $1O^{-3}$	6.4
# 4	0.000020	130	100	0.2000 x $1O^{-4}$	5.0
# 5	0.047250	160	160	0.6095 x $1O^{-3}$	14.6

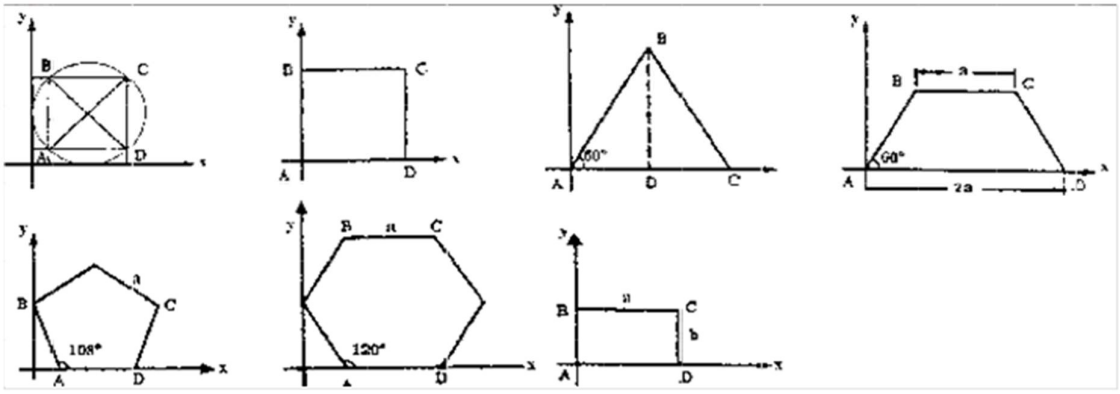

Figure 3. The shapes chosen in the real world are a, b, c, d, e, f, and g.

(iv) Once the mass-fraction outcome is inserted, the residual of the species continuity equation represents the remaining component of the equation. Generally, *R* is the sum of a times the

product of *nb* and *φnb*, plus b minus a times *φP*. *R* will be zero when the discretization equation is met.
The residual of mass-fractions is the change in mass-fraction values between two consecutive tries.
The final values found in this study were:
The leftover of the species continuity equation is 0. 2 times 10 to the power of negative 7.
The remaining amount is 0. 2 multiplied by ten to the power of negative two.
All reactors have different shapes in their cross-sections, but they all have the same length. The way we calculate things in these reactors is based on the amount of time the materials stay inside the reactor, or the size of the area in the cross-section. Also, we make sure that the speed of the materials entering the reactors is the same. The size of the circular tube in the situations being studied is displayed in Table 3.

The information from the analysis can be found in Tables 4 to 8. These tables present the findings obtained from studying five distinct cases. These tables show the average weight of the polymer in percentage, the molecular weights, and the polydispersity. It also indicates the temperature in degrees Celsius at the end of the reactors. The reactors show how much pressure is lost overall. These tables show that there are only small variations in the conversion results for different shapes in each scenario. Moreover, it has been observed that the specific shapes mentioned below are able to produce the highest conversion rate in each scenario.

Case number 1 involves a circular duct. The weight percentage of water per air in the duct is 6. 74%, and the pressure drop is 1. 46 Pascal Hexagonal duct is a pipe-like structure with a hexagon shape. It has a material called WPA which makes up 6. 74% of its weight. It also has a measurement called DP which is equal to 1. 69 Pascal
Case # 2: round tube with 14. 2% weight of water, Case # 3: round tube with 26. 6% weight of water.
In case number 4, we have a square duct with a weight percentage of 57. 2% and a pressure of 9078 Pa. We also have a circular duct with a weight percentage of 55. 2% and a pressure of 2617 Pa.
This is a case where we have a rectangular shape with an aspect ratio of 2:1. It has a weight percentage of 10. 70% and a pressure distribution of 106. 6 Pa
A circular tube with 10. 10% of water vapor mixed in the air and a pressure difference of 50. 8 Pascals

Table 3 The size across circular ducts that match with non-circular shapes.

Cases	**#1**	**#2**	**#3**	**#4**	**#5**
Diameter (m)	0.0400	0.0400	0.0110	0.0400	0.00460

Table 4 The results of a simulation that studied the process of styrene polymerization at the exit of a reactor are reported in this text. The simulation focused on one specific case, referred to as Case #1.

No	Geometry	WPA (wt %)	Mn (kg) kg mol	Mw (kg) kg mol	Polydispersity Mw / Mn	Bulk-Temp. (°C)	Total DP(Pa)
1	Circular	6.74	452460	819590	1.81	102.3	1.46
2	Square	6.74	452910	820240	1.81	102.2	1.88
3	Triangular	6.38	453450	820660	1.81	101.9	2.70
4	Trapezoidal	6.33	454100	822100	1.81	101.9	2.57
5	Pentagonal	6.63	453810	822110	1.81	102.1	2.28
6	Hexagonal	6.74	452940	820450	1.81	102.3	1.69
7	Rectangular (AR = 1.5)	6.70	453784	821697	1.81	102.0	1.91
8	Rectangular (AR = 2.0)	6.63	455120	823870	1.81	101.8	1.97

TABLE 5. Simulation Results of Styrene Polymerization at Reactor Exit: Case # 2.

No	Geometry	WPA (wt %)	Mn (kg) kg mol	Mw (kg) kg mol	Polydispersity Mw / Mn	Bulk-Temp. (°C)	Total DP(Pa)
1	Circular	14.2	338740	610770	1.8	106.0	1.05
2	Square	12.7	348550	628480	1.8	104.7	2.52
3	Triangular	11.0	351450	634420	1.8	103.7	6.11
4	Trapezoidal	11.3	352080	635670	1.8	103.7	6.36
5	Pentagonal	12.8	347180	625660	1.8	105.0	2.87
6	Hexagonal	13.6	343910	620230	1.8	105.4	2.76
7	Rectangular (AR = 1.5)	12.2	351620	634550	1.8	104.1	2.80
8	Rectangular (AR = 2.0)	11.5	356170	643600	1.8	103.3	3.26

TABLE 6. Simulation Results of Styrene Polymerization at Reactor Exit: Case # 3.

No	Geometry	WPA (wt %)	Mn (kg) kg mol	Mw (kg) kg mol	Polydispersity Mw / Mn	Bulk-Temp. (C)	Total DP (Pa)
1	Circular	26.6	220716	392673	1.78	136.3	243
2	Square	26.2	221160	393250	1.78	136.1	244
3	Triangular	24.8	220210	391120	1.78	136.0	347
4	Trapezoidal	25.4	220880	392530	1.78	136.0	347
5	Pentagonal	25.8	220420	391860	1.78	136.2	286
6	Hexagonal	26.5	220910	392960	1.78	136.2	254
7	Rectangular (AR = 1.5)	25.9	221278	393410	1.78	136.0	242
8	Rectangular (AR = 2.0)	25.8	221610	393980	1.78	135.9	261

TABLE 7. Simulation Results of Styrene Polymerization at Reactor Exit: Case # 4.

No	Geometry	WPA (wt %)	Mn (kg) kg mol	Mw (kg) kg mol	Polydispersity Mw / Mn	Bulk-temp (C)	Total DP (Pa)
1	Circular	55.2	481130	966680	2.00	101.4	2617
2	Square	57.2	499470	998160	2.00	101.2	9078
3	Triangular	47.4	486550	940300	1.93	101.1	11540
4	Trapezoidal	50.0	489210	953850	1.95	101.2	3625
5	Pentagonal	54.8	492120	979150	1.99	101.2	41568
6	Hexagonal	55.7	487320	976770	2.00	101.4	7574
7	Rectangular (AR = 1.5)	54.1	495730	979780	1.98	101.2	4937
8	Rectangular (AR = 2.0)	48.9	488230	947800	1.94	101.1	1910

TABLE 8 . Simulation Results of Styrene Polymerization at Reactor Exit: Case # 5.

No	Geometry	WPA (wt %)	Mn (kg)	Mw (kg)	Polydispersity Mw	Bulk-temp (C)	Total DP (Pa)

			kg□ mol	kg□ mol	___ □ Mn		
1	Circular	10.10	129960	225290	1.73	161.0	50.8
2	Square	9.97	130040	225440	1.73	160.9	67.2
3	Triangular	10.56	130330	225810	1.73	160.8	106.1
4	Trapezoidal	10.30	130380	226000	1.73	160.8	117.0
5	Pentagonal	10.20	130132	225600	1.73	160.9	67.8
6	Hexagonal	10.40	130100	225570	1.73	161.0	64.1
7	Rectangular (AR = 1.5)	10.20	130250	225810	1.73	160.8	73.9
8	Rectangular (AR = 2.0)	10.70	130430	226000	1.73	160.7	106.6

So, no particular shape is considered better than a circular duct reactor for getting the most conversion in a chemical reaction. This is also true for having the lowest pressure-drop. The reason why noncircular duct reactors have a higher-pressure drop is because of the corners, where the viscosity is very high. This was noticed by looking at the results of the viscosity profile.

Referring to Tables 4-8, the following classification is possible based on the circular duct results: Case # 1: 6. 74 percent Low conversion means that there is a low rate of success or effectiveness in turning potential customers into actual customers.
Case number 2: The content is 14. 20 percent by weight. few people buying
Case number 3: There is an intermediate conversion of 26. 60% by weight This is about Case number 4 where there is a high conversion rate of 55. 20 weight percent
Case number five: Ten point one zero weight percent low conversion. The cause of the low DP outcomes in cases number 1.

Number 2 happens because there is not a lot of change happening. The reason why case #5 has higher DP values, even at low conversion level, is because it has a smaller tube inner diameter. In this case, the measurement practiced was 0. 0046 meters in this section, we show results of simulations which tell us about the sizes of molecules, how fast they move, how hot or cold they are, how concentrated they are, how tightly packed they are, and how sticky they are. These results are shown as pictures from Figure 4 to Figure 15.

When we look closely at these numbers, we can see a few important things.
MOL is short for "Moment of Love". Weight All cases, except Case #4 which has high conversion, show a peak that is closer to the entrance of the reactor. In situation number 4, there is a. A slow and steady rise in the weight of an object. The movement of something from the starting point to the final point in the reactor. The results are not clear enough to make a conclusion that applies to everyone. The reason for the peak is that the temperature is more

even across places that are closer to the reactor's entrance. This leads to the production of very good quality polymer. As you move further downstream, the heat from the reaction at the center of the ducts builds up, causing the temperature to be uneven across the width of the ducts. This uneven temperature negatively affects the quality of the polymer. This means that the weight of particles becomes less as they move downstream. A typical MOL is an average example or representation of something.

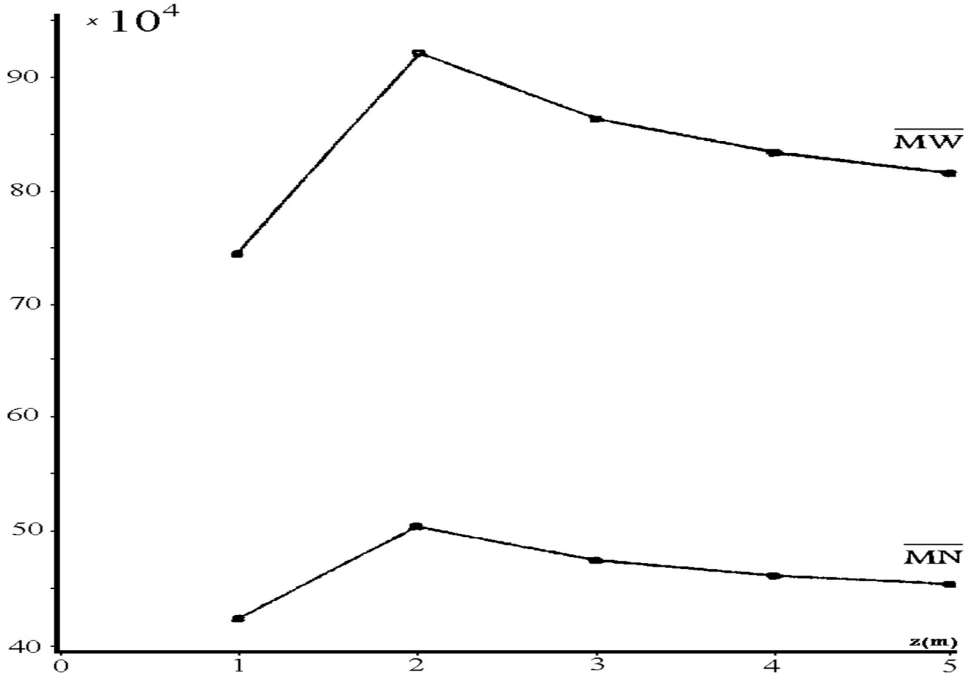

Figure 4. Case#1 mol. wt distribution (triangle).

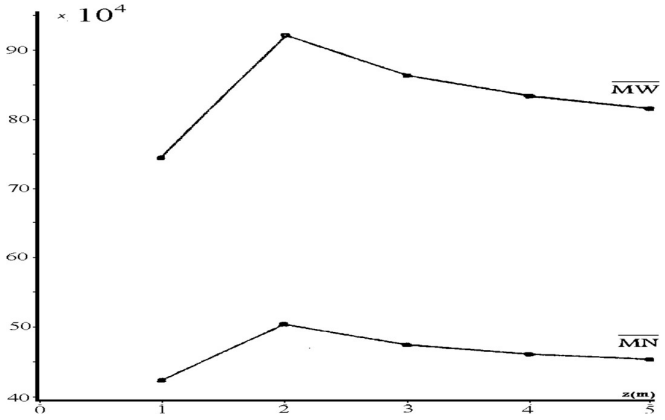

Figure 5. Case#1 mol. wt distribution (trapezoid).

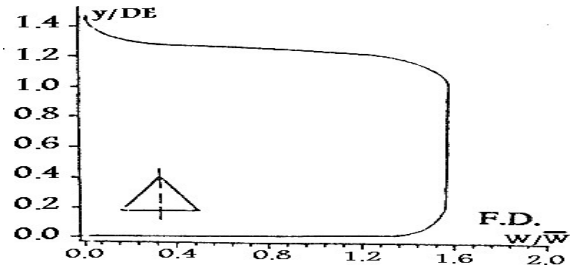

Figure 6. Case#1 axial-velocity profile (triangle).

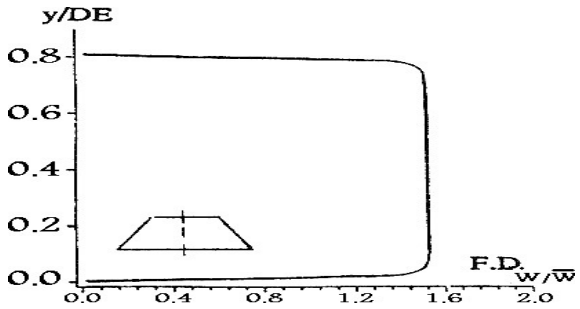

Figure 7. Case#1 axial-velocity profile (trapezoid).

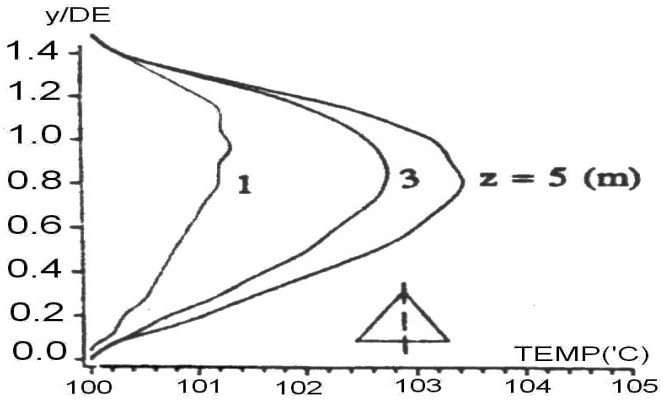

Figure 8. Case#1 temperature profile (triangle).

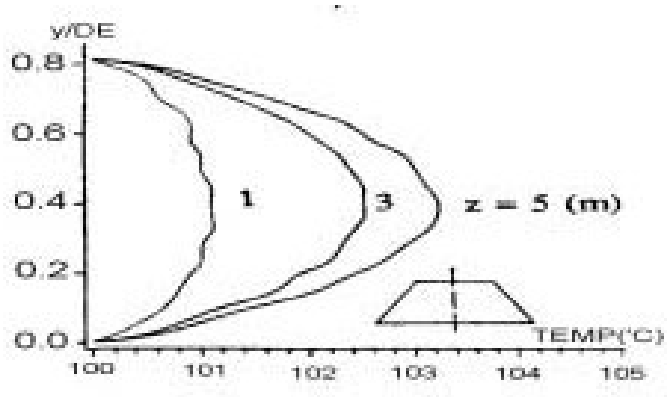

Figure 9. Case#1 temperature profile (trapezoid).

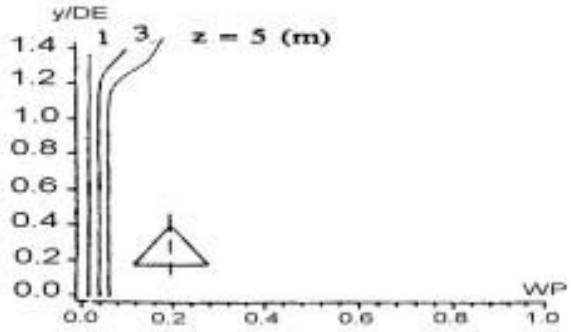

Figure 10. Case#1 polymer-concentration profile (triangle).

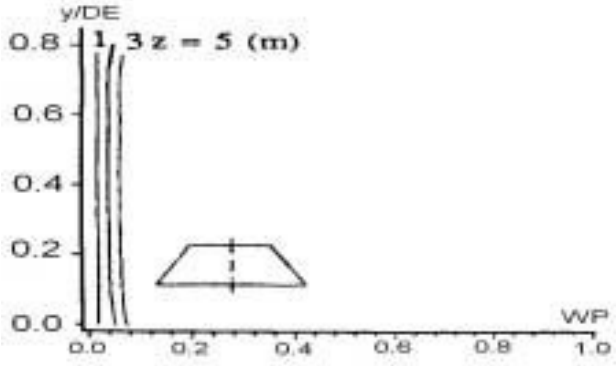

Figure 11. Case#1 polymer-concentration profile (trapezoid).

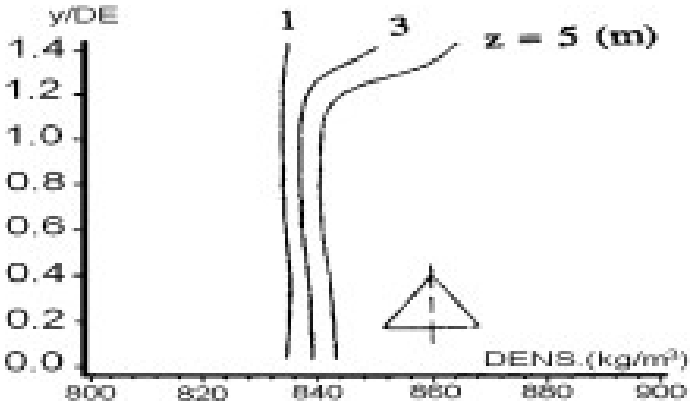

Figure 12. Case#1 density-profile (triangle).

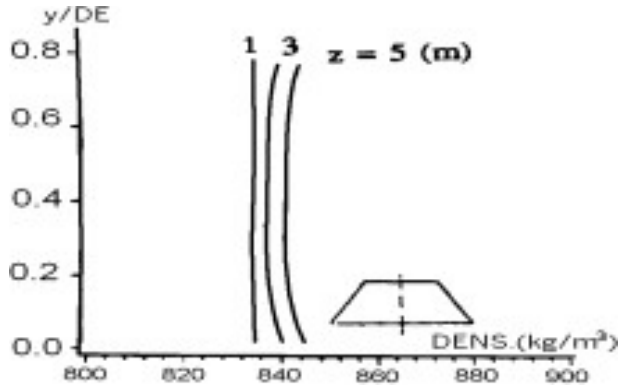

Figure 13. Case#1 density-profile (trapezoid).

The speed of flow in all cases is consistent with the pattern expected by Hussain and Hammered [3]. We can see that there is a change in speed caused by angles, specifically in ducts shaped like triangles or pentagons. This effect causes more polymers to be made at the corners instead of the sides, which makes the liquid thicker near the angles. The speed slows down near the angles. You can see typical speed profiles in Figures 7 and 8 for triangular and trapezoidal duct reactors.

(iii) Temperature Profiles (iii) How hot or how cold an object or a place is.
Situation #1: In a reactor, a chemical reaction that gives off heat is happening, and the temperature is increasing.
In the second case, we are using a cooled-wall reactor where we can see heat being removed. This is happening because the temperature is getting lower.
Case number 3 is about a reactor where the temperature is gradually decreasing.
In this fourth case, the reactor with a cooled wall is experiencing a decrease in temperature as time goes on.
Case #5: In a special type of reactor, the temperature is increasing.
The temperature patterns commonly found in triangular and trapezoidal duct reactors are displayed in Figures 8 and 9.

The concentration levels are changing and forming profiles. Talking about angles, like in triangular and pentagonal ducts, we see that there is more stuff concentrated there. The quantities of a substance in reactors resembling triangles and trapezoids can be observed in Figures 10 and 11.

The way angles affect the thickness of a liquid is clear in the profiles that show a big increase in thickness near the angles. This is seen in the thickness patterns for the triangular and pentagonal tubes of every situation. The density patterns are also slightly changed near these areas. The angle effect is what causes noncircular duct reactors to have a higher pressure-drop compared to circular ones. The regular density and thickness variations in triangular and trapezoidal duct reactors are illustrated in Figures 12 to 15.

The impact of buoyancy, known as free-convection, is negligible in this research due to the limited temperature range. This information is based on the results we found when studying the free-convection effect in circular ducts. We looked at the results in Tables 4-8 to come to this conclusion.

Case # 1: 6.75 wt % conversion.
Case # 2: 14.50 wt % conversion.
Case # 3: 26.70 wt % conversion.
Case # 4: 55.24 wt % conversion.
Case # 5: 10.30 wt % conversion.

SUMMARY AND CONCLUSIONS

This study explains how a particular method can be used to solve equations related to fluid flow and chemical reactions in duct reactors. The method involves transforming the coordinates in a way that fits the shape of the boundaries. The good agreement between our method and other researchers' results for round ducts and the fact that there were no problems with reaching a solution show that our method is very effective. The above solution technique is used to study how styrene polymerization occurs in duct reactors with different shapes. We have noticed that no particular shape is always better than the traditional circular duct reactors, especially when considering the lowest pressure drop in the reactors.

REFERENCES

1. Sala, R., Valz-Gris, F. and Zanderighi, L., “A Fluid-Dynamic Study of a Continuous Polymerization Reactor”, Chemical Engineering Science, 29, (1974), 2205-2212.
2. Wyman, C. E. and Carter, L. F., “A Numerical Model for Tubular Polymerization Reactors”, AIChE Symposium Series, Vol. 72, No. 160, (1976), 1-16.
3. Husain, A. and Hamielee, A. E., “Bulk Thermal Polymerization of Styrene in a Tubular Reactor—a Computer Study”, AIChE Symposium Series, Vol. 72, No. 160, (1976), 112-127.
4. Hui, A. and Hamielee, A. E., “Thermal Polymerization of Styrene at High Conversions and Temperatures, An Experimental Study”, J. Appl. Polymer Science, 16, (1972), 749-762.
5. Valsamis, L. and Biesenberger, J. A., “Continuous Bulk Polymerization. in Tubes”, AIChE Symposium Series, Vol. 72, No. 160, (1976), 18-27. Flow Heat and Mass Transfer in

Ducts of Arbitrary Cross- Sections for Power-Law Fluids", Ph.D. Thesis, McGill University, Montreal. Canada, (1993).

12. Bird, R. B., Stewart, W. E. and Lightfoot, E. N., "Transport Phenomena", Wiley, New York, (1960).

13. Skelland, A. H. P., "Non-Newtonian Flow and Heat- Transfer", John Wiley and Sons, NY., (1967).

14. Chu, W. H., "Development of a General Finite Difference Approximation for a General Domain", J. Comp. Physics, 8, (1971), 392 -408.

15. Thompson, J. F., Thames, F. C. and Mastin, C. W., "Boundary-Fitted Curvilinear Coordinate Systems for Solution of Partial Differential Equations on Fields Containing Any Number of Arbitrary Two-Dimensional Bodies", Report CR-2729, NASA Langley Research Center, (1977).

16. Maliska, C. R. and Raithby, C. D., "A Method for Computing Three Dimensional Flow Using Non-Orthogonal Boundary— Fitted Coordinates", Int. J. for Numerical Methods in Fluids, 4, (1984), 519-537.

17. Patankar, S. V. and Spalding, D. B., "A Calculation Procedure for Heat, Mass and Momentum Transfer in Three- Dimensional Parabolic Flows", Int. J. Heat Mass Transfer, 15, (1972), 1787-1806.

18. Patankar, S. V., "Numerical Heat Transfer and Fluid Flow", Hemisphere Publishing Corporation, NY., (1980).

19. Raithby, G. D. and Schneider, G. E., "Numerical Solution of Problems in Incompressible Fluid Flow: Treatment of the Velocity-Pressure Coupling", Numerical Heat Transfer, 2, (1979), 417-440.